

THE ADHESION OF NICKEL USING AN ION BOMBARDMENT  
AND HEATING CLEANING TECHNIQUE

by

James M. Bradford, Jr.

NASA, Langley Research Center  
Hampton, Virginia

To be presented at the 1968 Vacuum Metallurgy Conference  
June 10-13, 1968  
Beverly Hills, California

GPO PRICE \$ \_\_\_\_\_  
CSFTI PRICE(S) \$ \_\_\_\_\_

Hard copy (HC) 3.00  
Microfiche (MF) 1.65

Sponsored by:  
The Vacuum Metallurgy Division  
American Vacuum Society

# 653 July 65

N 62-34797  
(ACCESSION NUMBER)

(THRU)

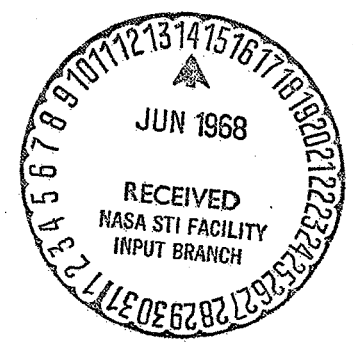
FACILITY FOR

22  
(PAGES)

(CODE)

Tmx 61229  
(NASA CR OR TMX OR AD NUMBER)

15  
(CATEGORY)



## INTRODUCTION

The adhesion of metal surfaces is the controlling parameter in many industrial metal joining techniques. Metal cladding, ultrasonic welding, and friction welding all depend upon the adhesion of the metal surfaces to provide the joining force. It has been discovered that the surface oxides on most metals must be disrupted or removed before the bonding will occur. This disruption is usually accomplished by some mechanical process such as scratching or deforming the surface. In these processes high deformation rates are used and sometimes the metals are joined while at high temperature. It has been shown,<sup>1</sup> however, that if the surfaces are sufficiently clean when they are put into contact, it is possible to achieve adhesion between some metal surfaces using small contact forces and without the need for high contact temperatures. This paper presents the results of an investigation of such clean surfaces wherein the effects of oxygen recontamination, contact force, hardness, and temperature on the adhesion coefficient were studied.

## DESCRIPTION OF APPARATUS

The apparatus of interest used during this investigation were: (1) an ultrahigh vacuum chamber which was used to provide the correct environment for the investigation, (2) a motor-driven linear motion feedthrough which was used to bring the samples into contact to make the adhesion couple and to move the samples apart to break the couple, (3) the samples which were machined from polycrystalline nickel rod, and (4) an electron gun which was used in the cleaning procedure to clean the sample surfaces.

The samples and some of the other apparatus had to be installed in the ultrahigh vacuum chamber to provide a very low-pressure environment so that once the samples had been cleaned, they would remain clean long enough to be investigated in the clean condition. The ultrahigh vacuum chamber was a horizontal cylinder 30 inches in diameter and 42 inches long. The vacuum chamber and the experimental apparatus are shown in figure 1. The vacuum chamber was pumped by a 10-inch oil diffusion pump which was backed by a 2-inch diffusion pump and a mechanical roughing pump. A water-cooled baffle and a liquid nitrogen baffle were located between the diffusion pump and the vacuum chamber to prevent oil backstreaming. The pressure in the chamber after it had been baked and with the experimental apparatus installed was about  $5 \times 10^{-10}$  torr. More details about the vacuum chamber and the experimental apparatus used in this investigation are given in reference 2.

The motor-driven linear motion feedthrough is also shown in figure 1. The variable-speed motor actuated a screwjack which, in turn, actuated the linear motion feedthrough. One of the test samples (left sample) was attached to the end of this linear motion feedthrough that was inside the vacuum chamber. The other sample (right sample) was fixed in place inside the vacuum system. The left sample could then be moved in or out to make or break the adhesion couple. A strain gage mounted on the linear motion feedthrough inside the vacuum chamber was used to measure the forces involved in this investigation.

The samples are shown in figure 2. They were machined from very pure polycrystalline nickel rod and were threaded on one end to facilitate mounting. The tip of the left sample was approximately 0.1 inch in diameter.

This diameter controlled the area in contact between the samples. A closeup of the samples installed in the chamber is shown in figure 3. The left sample holder is mounted on the end of the linear motion feedthrough and the right sample holder is fixed inside the chamber.

The electron gun used in the cleaning procedure is also shown in figure 3. The magnet shown in the figure provided an axial magnet field around the gun and the reflector electrode increased the path length of the ionizing electrons during the ion bombardment procedure. More about the electron gun is given below.

#### PROCEDURE

The procedure used to conduct the adhesion tests was: first, to clean the sample surfaces; second, to bring the samples into contact with a prescribed contact force to form the adhesion couple; and third, to pull the samples apart and measure the force required to break the adhesion couple. The cleaning procedure consisted of outgassing the samples at 550° C for one hour and then alternately ion bombarding and heating the samples for five cycles. Both the ion bombardment and heating parts of the cleaning cycle were accomplished using the electron gun already discussed.

During the ion bombardment cycle argon was admitted into the back of the electron gun. The argon then flowed through the electron gun and as it passed through the gun it was ionized by the electrons being emitted from the filament. The argon ions were then accelerated into the samples which were biased at minus 2000 volts during the ion bombardment. The ion dosage during

each ion bombardment cycle was approximately  $4 \times 10^{-3}$  coulombs per square centimeter front surface.

During the heating part of the cleaning cycle electrons from the electron gun impinged upon the samples which were then biased at plus 1000 volts. The electron gun was designed so that there was not a straight line path from the electron gun filament to the samples when the samples were positioned as shown in figure 3. Thus the samples were shielded from possible tungsten contamination from the filament. The duration of each heating cycle was 15 minutes.

After the samples had been cooled to the test temperature (which, unless otherwise specified, was room temperature) they were put into contact by traversing the left sample inward. After a predetermined time at a predetermined contact force the left sample was traversed outward and the force required to break the adhesion couple was measured.

One of the fundamental parameters in adhesion testing is the adhesion coefficient. It is defined as the breaking force divided by the contact force and will be used in the presentation of the data from this investigation.

#### SURFACE CHARACTERIZATION

It was stated above that this would be an investigation of clean surfaces. The method used to determine that the surfaces were clean has been reported in an earlier report<sup>2</sup> and will not be discussed here. However, some confidence that the surfaces are clean can be obtained simply by recontaminating the clean surface with oxygen. If the surfaces were clean before the oxygen

was sorbed on the surface, then from previous investigations,<sup>3, 4</sup> the adhesion coefficient should decrease even for low oxygen coverage.

The dependence of the adhesion coefficient upon oxygen recontamination was measured. The samples were cleaned and then exposed to oxygen for a specified time at a specified pressure. The adhesion coefficient was then measured, the surface was recleaned and exposed to a higher oxygen exposure, and the adhesion coefficient again measured. By repeating such tests the variation of the adhesion coefficient with oxygen exposure was measured and is shown in figure 4.

The results showed that the adhesion coefficient decreased from 0.36 at zero exposure to 0.27 at about  $2 \times 10^{-7}$  torr-seconds exposure. If we assume a sticking coefficient of unity for up to single monolayer coverage, the partial monolayer coverage can be calculated from the exposure and is shown along the top of figure 4. Thus the adhesion coefficient decreased for coverages as low as one-tenth of a monolayer. This decrease indicates that the clean surface was indeed relatively free from oxygen contamination. The adhesion coefficient continued to decrease as the exposure to oxygen was increased and decreased to zero when the oxygen exposure was about  $10^{-4}$  torr-seconds. This decrease of the adhesion coefficient with increased oxygen exposure is the same effect that is observed when contaminated surfaces fail to adhere as well in air as the surfaces that have been cleaned in some fashion.

## RESULTS AND DISCUSSION

Hardness.- The variation of the adhesion coefficient with sample hardness before putting the samples into contact was measured. The samples were cleaned and put into contact with a contact force approximately equal to the force necessary to cause compressive yielding of the samples. The breaking force was then measured and the samples put into contact again without an interim cleaning procedure. The spot of metal in contact at the adhesion junction was strain hardened during each adhesion test. As the testing proceeded without any interim cleaning procedure (which annealed the samples during the heating period) the metal in contact became hardened. Thus the hardness of the samples was varied by strain hardening the metal in contact. The hardness of the samples in the vacuum chamber was duplicated by subjecting a sample outside the vacuum chamber to the same deformations and measuring its change in hardness.

The variation of the adhesion coefficient with hardness is shown in figure 5. In general, there is an inverse relationship between the adhesion coefficient and the hardness. This variation has been discussed in the literature but these discussions have been limited to the variations of hardness and adhesion coefficients between different metals from indium to aluminum.

This inverse relationship between the hardness and the adhesion coefficient is usually explained in terms of the increased area in contact for the softer metals. Thus if a metal is softer there is more area in contact and thus more adhesion. This simplistic correlation is limited by two observations. The first is that the hardness is also a measure of the compressive

yield strength, and although the softer metals have more area in contact, they are also weaker which should offset the increase in the adhesion coefficient caused by the increased area in contact. The second observation is that all soft metals do not have high adhesion coefficients (e.g., magnesium and zinc).<sup>5</sup>

Contact force.- The variation of the force required to break the adhesion couple with the contact force was measured and is shown in figure 6. The samples were cleaned and pressed together with various contact forces from 10 pounds to 300 pounds. The samples were cleaned prior to each test. The breaking force increased with increasing contact force over the entire range tested. The scatter in the data below 150 pounds contact force is probably due to some variation in the hardness between the tests. A contact force of 150 pounds was approximately the force required to cause compressive yielding of the nickel. Thus the tests in which the samples were pressed together at contact forces greater than compressive yielding show less scatter because the samples were all strain hardened by the contact force to some relatively constant value.

Deformation ratio.- If the data in figure 6 are replotted as shown in figure 7, the influence of the compressive yield strength upon the adhesion coefficient is shown. Figure 7 shows the variation of the adhesion coefficient with the deformation ratio which is the contact stress divided by the compressive yield strength. The adhesion coefficient was relatively constant in the range from 0.1 to 0.3 for deformation ratios from 0.02 to about 1. For deformation ratios greater than 1, the adhesion coefficient increased with increasing deformation ratio. At the highest deformation ratio tested



the adhesion coefficient is greater than 1 which means that the breaking force was higher than the contact force. The breaking stress at this deformation ratio is approximately one-third the tensile strength of the virgin material.

There have been many measurements of the effect of the normal load on the adhesion coefficient. Most of these measurements supported the so-called "law of adhesion" which states that the adhesion coefficient is independent of the load. The data in figure 7 show that the adhesion coefficient for nickel was independent of the load only for deformation ratios less than unity. For larger deformation ratios, the adhesion coefficient increased with increasing load.

Temperature during time in contact.- The dependence of the adhesion coefficient upon the temperature during time in contact was measured. The samples were cleaned and put into contact after they had cooled to room temperature. The temperature was then increased and the samples held at the desired temperature for 1 hour. The samples were then cooled to room temperature and the breaking force measured. The results of a series of these tests is shown in figure 8. The adhesion coefficient was about 0.2 from room temperature to about 200° C at which point the adhesion coefficient starts increasing. The adhesion coefficient then increases sharply with increasing temperature up to the highest temperature tested which was about 530° C. The shape of the curve suggests that an equation of the form

$$\alpha = \alpha_0 + Ae^{-Q/RT} \quad (1)$$

would fit the data. The equation is a modification of an equation proposed

by Ling.<sup>6</sup> The agreement between the data and equation (1) is shown on figure 8. The constants used in equation (1) are listed in table I.

It is interesting to note that the value of  $Q$  in table 1 is approximately the same as values in the literature for the activation energies for surface diffusion of nickel. The increase in the adhesion coefficient could then be due to an increase in the area in contact between the samples.

#### SUMMARY

In summary of the results of this investigation, a number of conclusions can be drawn. First, the ion bombardment-heating cleaning technique can be used to study the adhesion of clean nickel surfaces. Second, the adhesion coefficient of the clean surface is reduced by even partial monolayer coverage of oxygen and decreases to zero at an oxygen exposure of about  $10^{-4}$  torr-seconds. Third, the adhesion coefficient is inversely dependent upon the hardness of the nickel sample. Fourth, the adhesion coefficient is relatively constant at about 0.2 for deformation ratios less than unity and increases with increasing deformation ratio for deformation ratios greater than unity. Finally, the dependence of the adhesion coefficient upon the temperature is given by equation (1) where the activation energy is comparable to the activation energy of surface diffusion of nickel on nickel.

## REFERENCES

1. Johnson, R. E., and Keller, D. V., Jr., J. Vac. Sci. and Tech., 4, 115, (1967)
2. Bradford, J. M., Jr., "A Study of the Adhesion of Nickel," Dissertation, North Carolina State University, Raleigh, North Carolina (1968)
3. Gilbreath, W. P., and Sumsion, H. T., J. Spacecraft Rockets, 3, 674-679, (1966)
4. Keller, D. V., Jr., "On the Analysis of Adhesion Data," ASTM-STP-431, (1967)
5. Sikorski, M. E., Wear, 7, 144-162, (1964)
6. Ling, F. F., "Welding Aspect of Sliding Friction Between Unlubricated Surfaces," AFOSR-TR-60,117, ASTIA, (1960)

Table I. Constants in equation (1)

$\alpha_0$	0.22
A	23,232
Q	$15 \frac{\text{k cal}}{\text{gm mole}}$
n	$\approx 0$

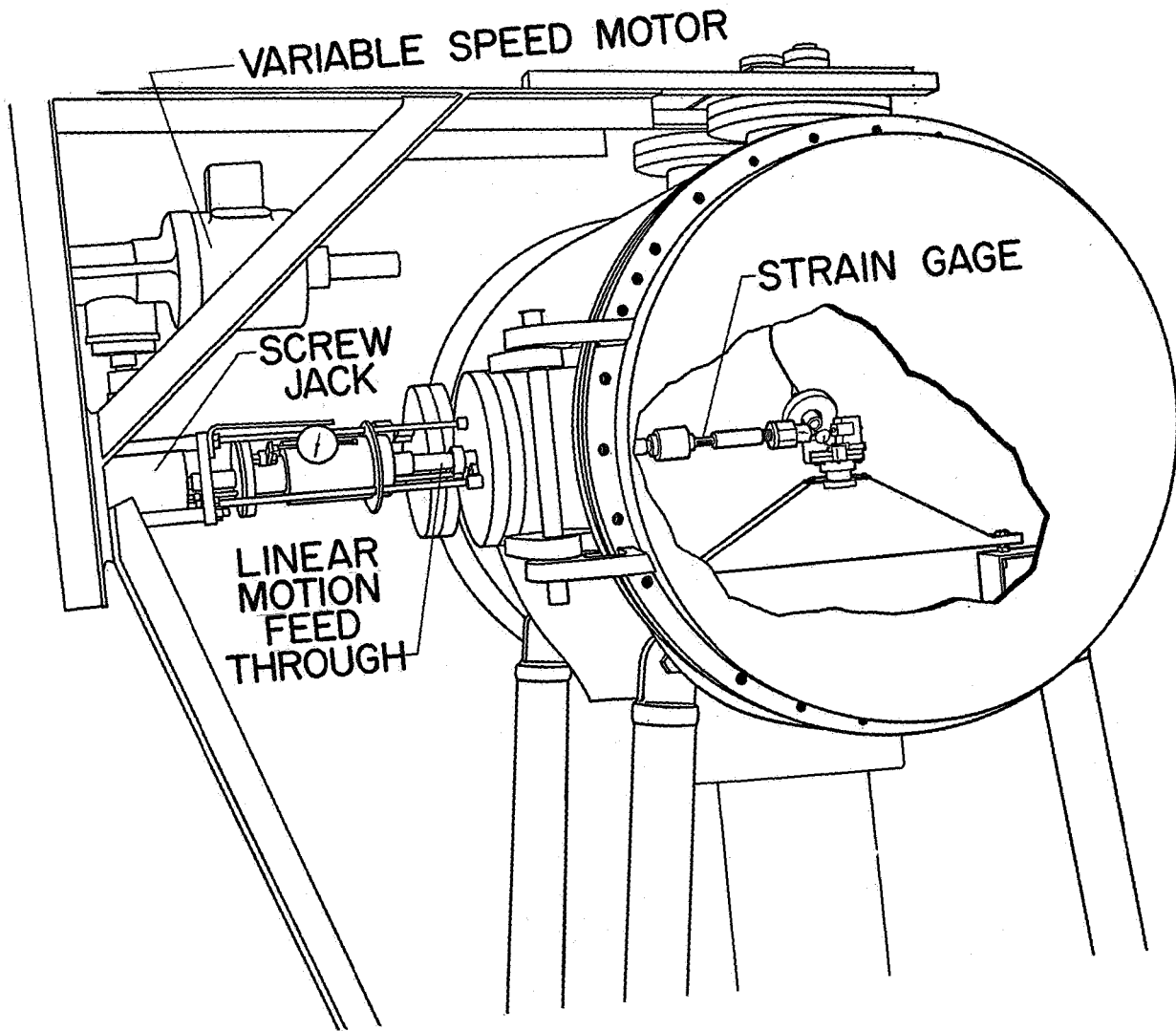


Figure 1.- Experimental apparatus.

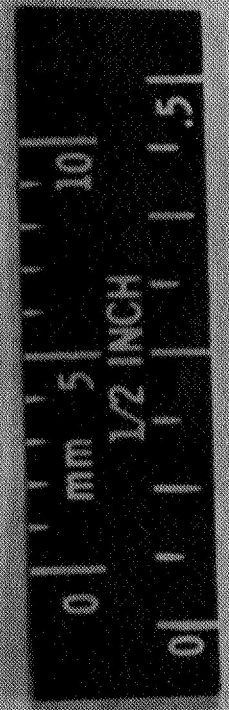
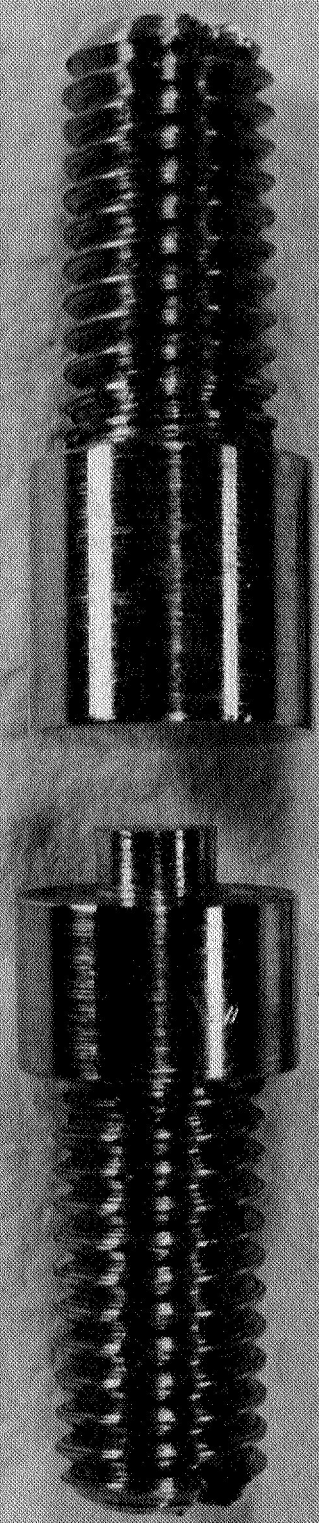
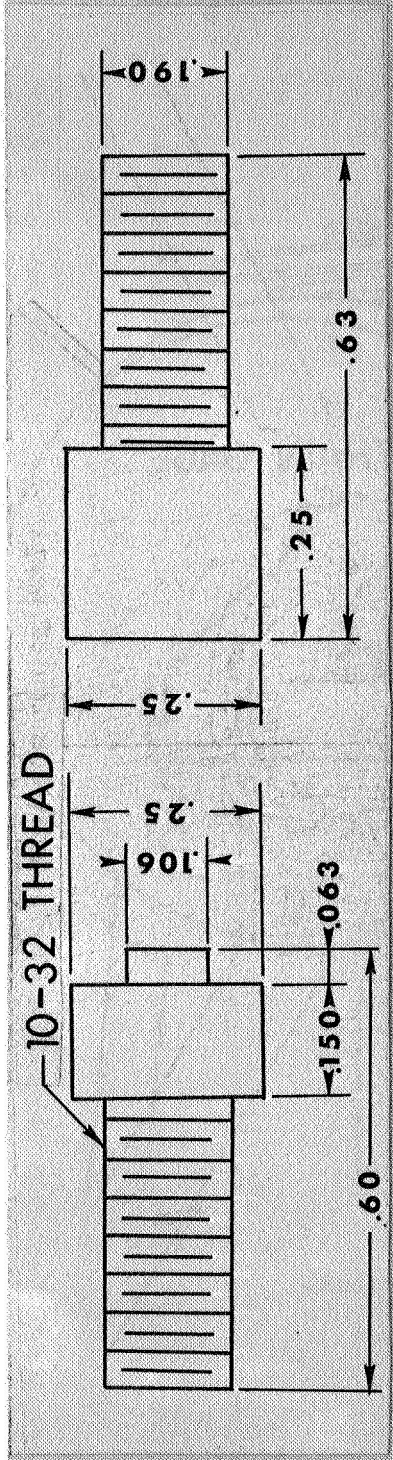


Figure 2.- Set of samples.

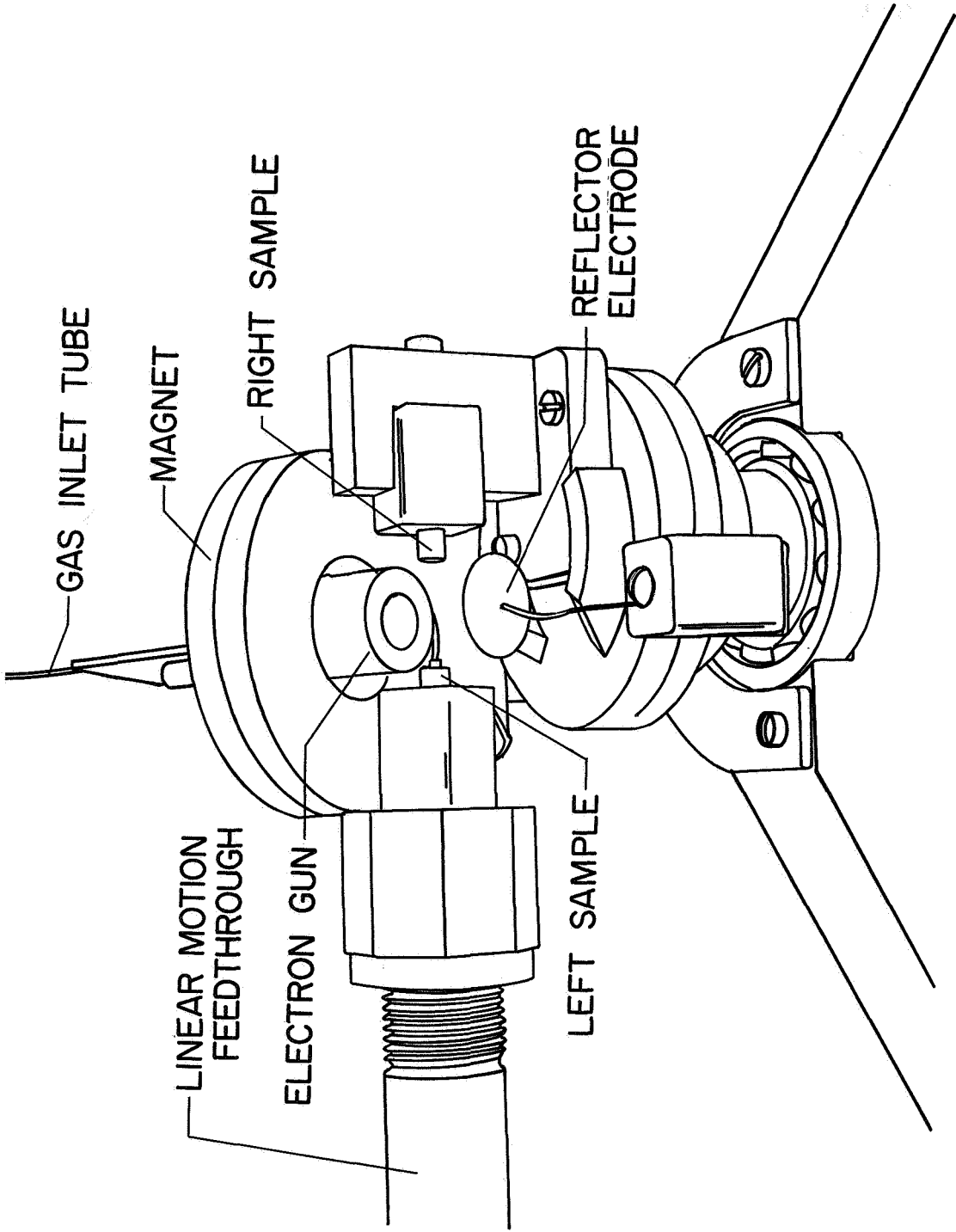


Figure 3.- Installation of samples.

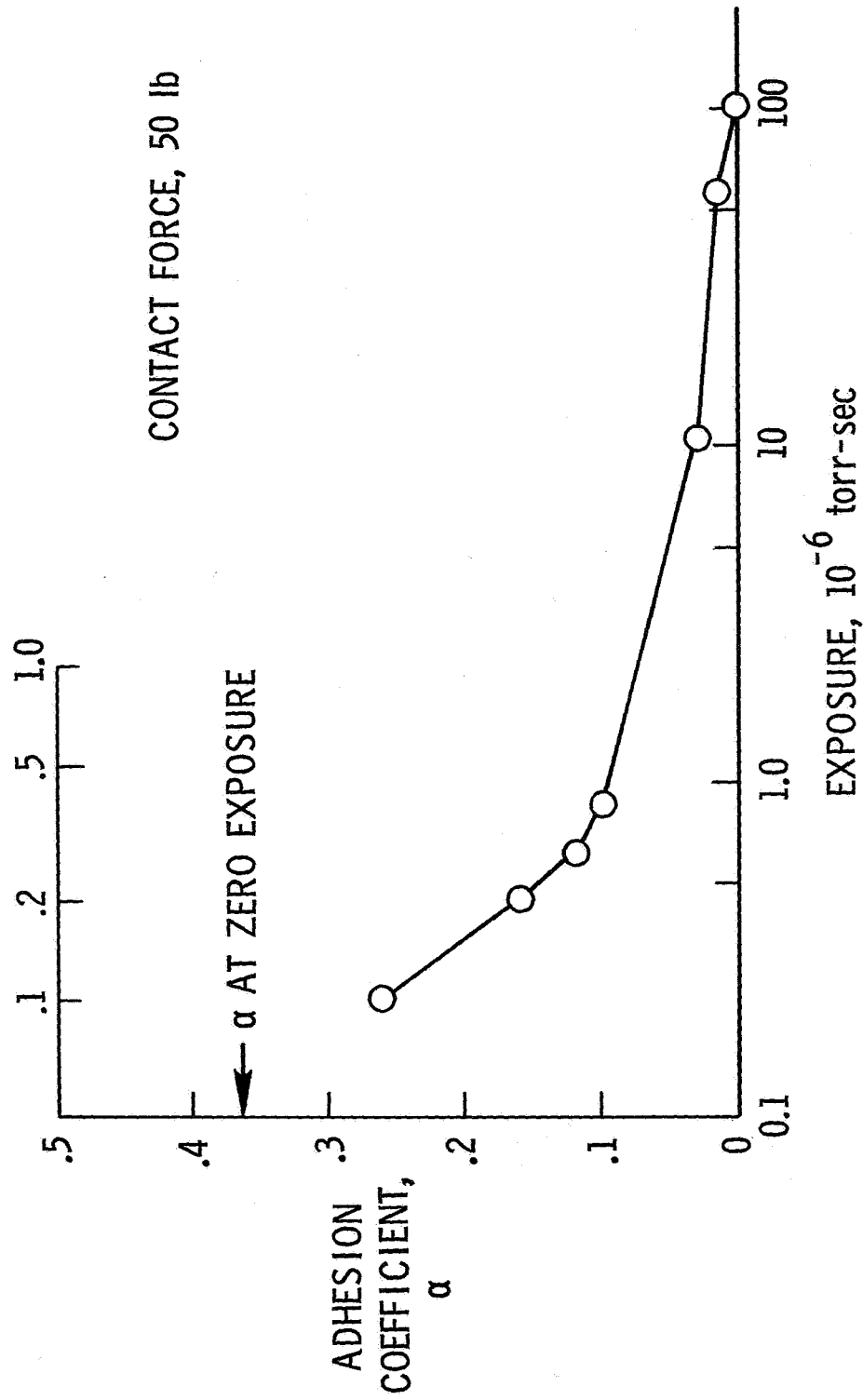


Figure 4.- Variation of adhesion coefficient with oxygen exposure.



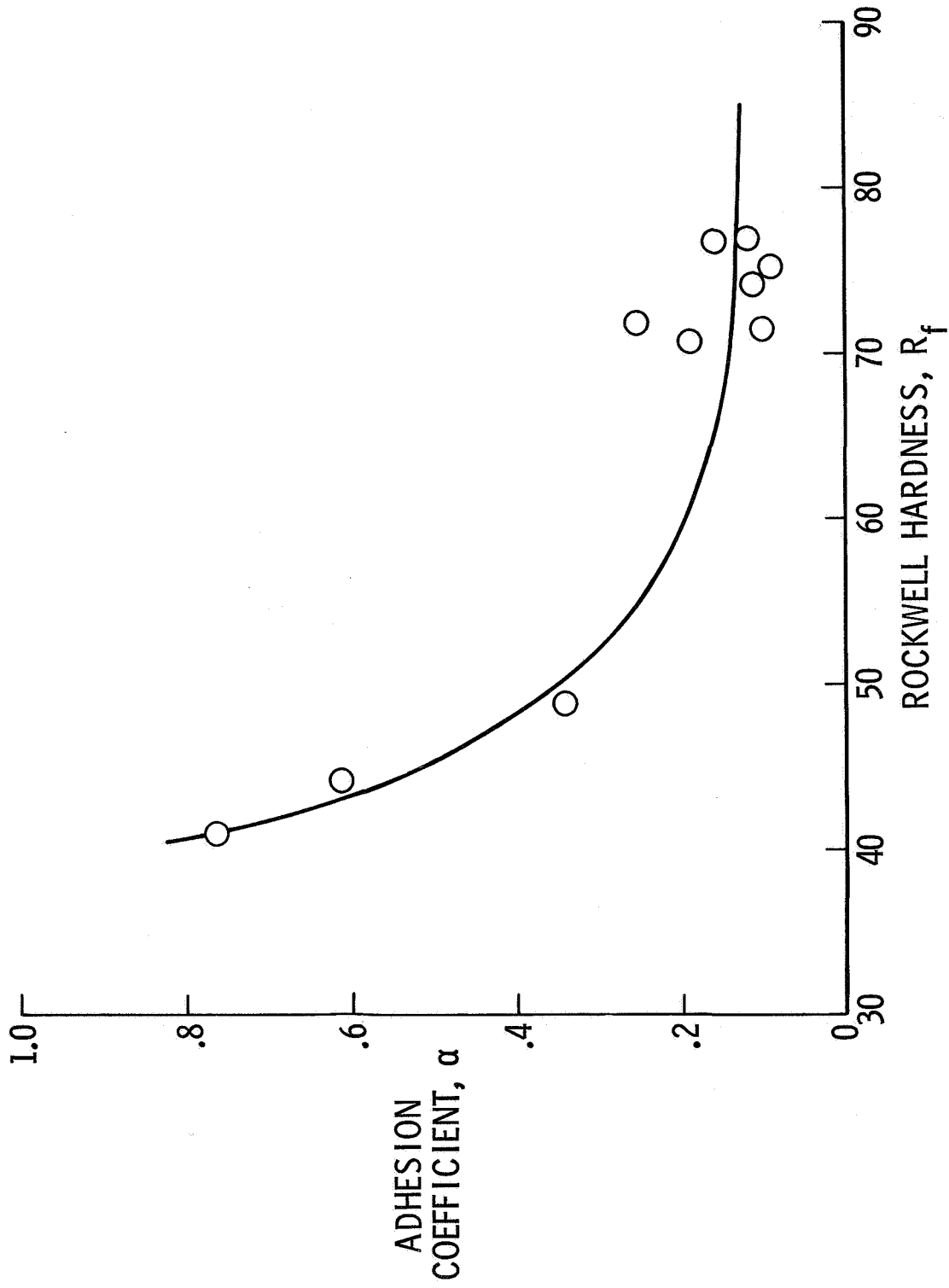


Figure 5.- Variation of adhesion coefficient with hardness.

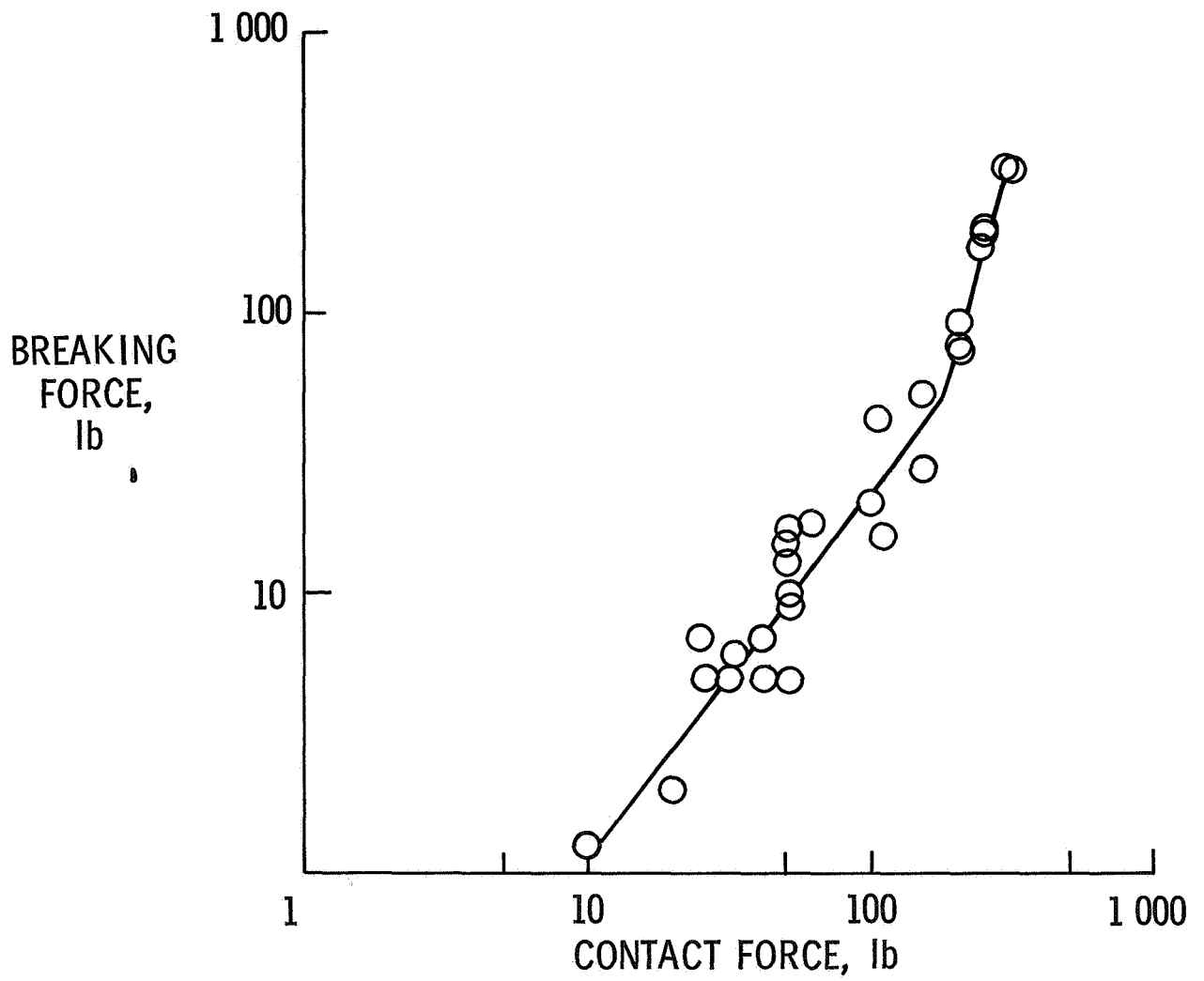


Figure 6.- Variation of breaking force with contact force.

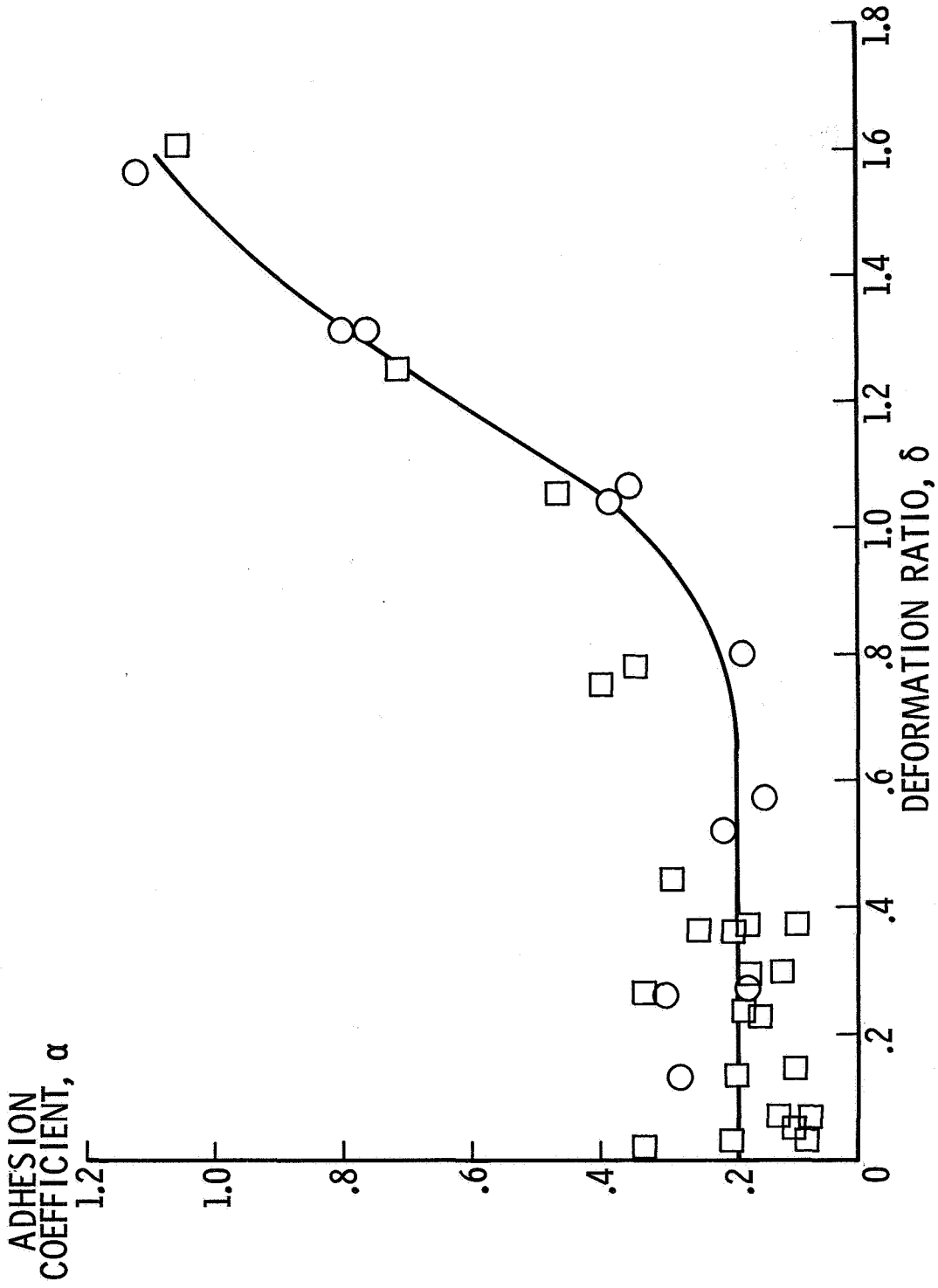


Figure 7.- Variation of adhesion coefficient with deformation ratio.

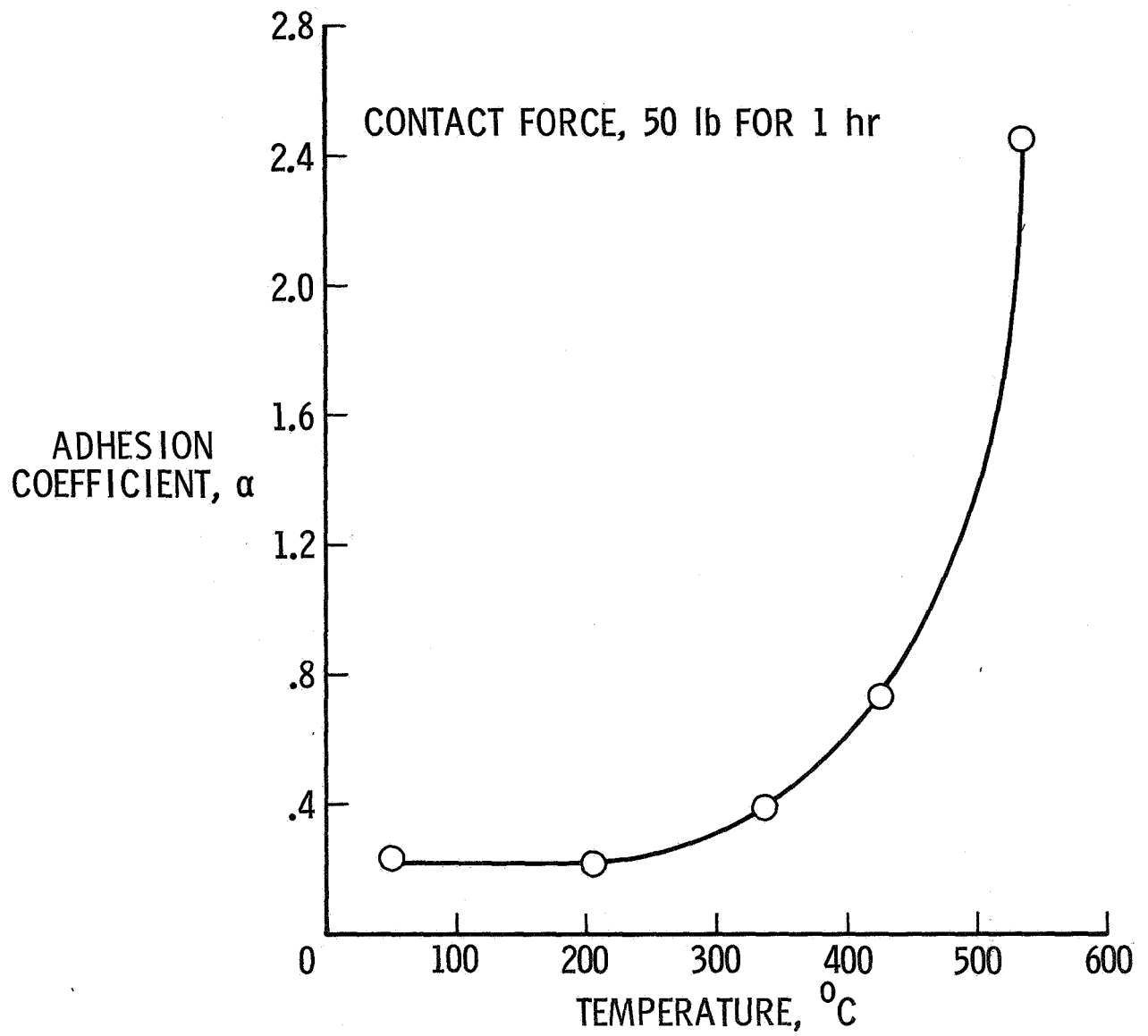


Figure 8.- Variation of adhesion coefficient with temperature during contact.

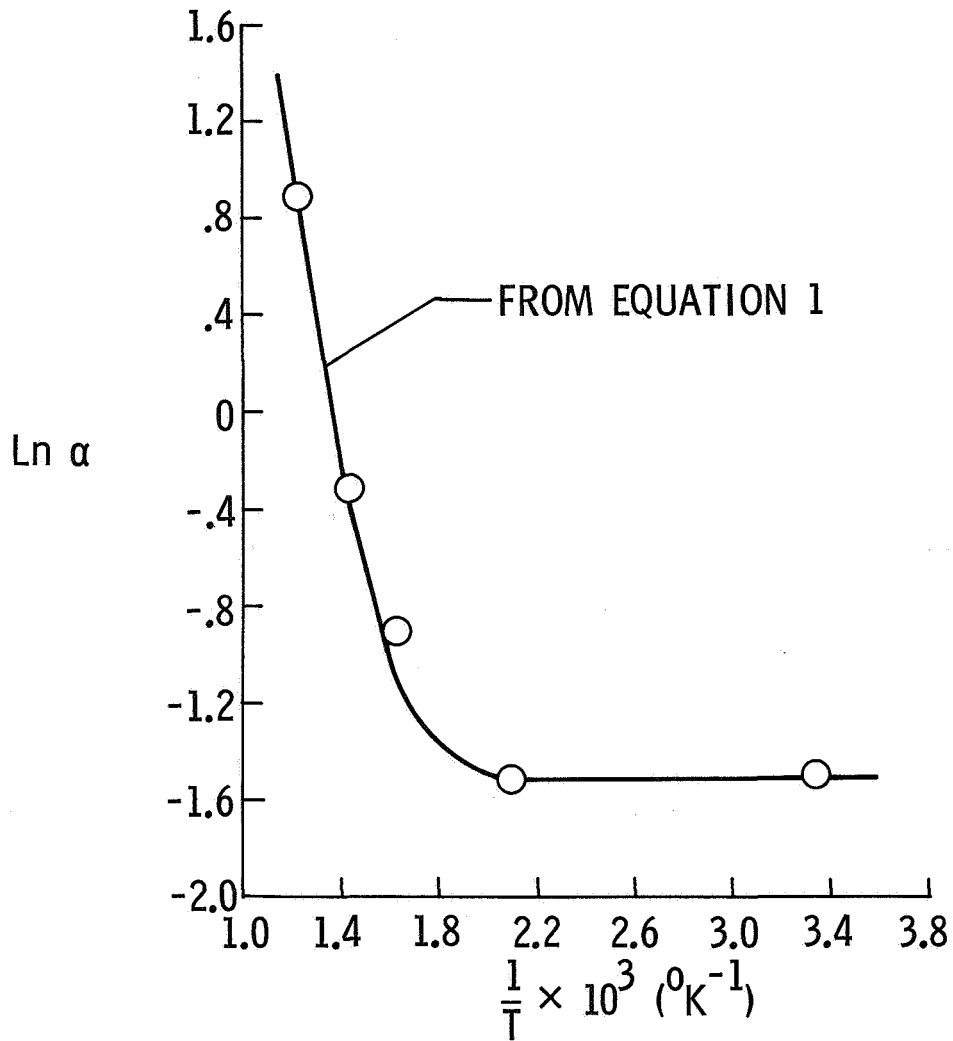


Figure 9.- Comparison of experimental data with equation 1.